

# DESIGN METHOD FOR PROTOTYPING A COST-EFFECTIVE VR SPHERICAL MOTOR

Kok-Meng Lee, Jeffrey Joni and Hungsun Son  
The George W. Woodruff School of Mechanical Engineering  
Georgia Institute of Technology  
Atlanta, GA, 30332-040  
Email: [kokmeng.lee@me.gatech.edu](mailto:kokmeng.lee@me.gatech.edu)

**Abstract-** This paper presents a CAD/CAE procedure for designing a variable-reluctance spherical motor (VRSM). The procedure offers an effective way to optimize key parameters that could significantly affect the torque performance of a VRSM. Specifically, the analytical procedure streamlines the design process using a conceptual design as an input to create 3D solid models, upon which FE analyses are performed to optimize key parameters. As an illustrative example, we introduce the design concept of a SWM capable of open-loop orientation control while its rotor spins continuously and demonstrate the concept feasibility experimentally.

## I INTRODUCTION

Precision-motion actuators with multi degrees-of-freedom (DOF) have found many applications in the modern industries. One such actuator is a ball-joint-like spherical motor capable of offering three-DOF in a single joint. Spherical motors take a number of forms which include the induction motors [1] [2], the direct-current motors [3] [4] [5], the stepper [6] [7]; the variable-reluctance motors [8] [9] and the ultrasonic motor [10]. Compared with its counterpart, a spherical stepper has a relatively large range of motion, possesses isotropic properties in motion, and is relatively simple and compact in design. This provides an incentive for further development.

The basic concept of a spherical stepper was originally proposed by [6]. The dynamic model of a particular VRSM can be found in [8], where the torque model is a quadratic function of the current inputs to the stator electromagnets (EM's). More recently, the interest to derive a closed-form solution to the inverse torque model has led [11] to design a VRSM that has a linear torque-current relationship. In this paper, we present a numerical procedure based on computer aided design (CAD) and finite element (FE) analysis to streamline the design process and reduce development time of a new prototype. The numerical process, as illustrated in Fig. 1, begins with a set of requirement specifications followed by generating a 3D solid model of the conceptual design. The parameters that affect the motion are identified and then modeled in FE software [12] [13] for further analysis. Written in MATLAB, a FE command file (in this case ANSYS APDL) is written to compute quasi-statically the torque of a VRSM for a specified range of separation angles. The results are then plotted to determine the optimal parameters of the design. A final 3D solid model of the prototype is then generated.

Finally, the new prototype is fabricated and its performance is tested.

Specifically, this paper offers the following:

- (1) We present a particular design of VRSM design, referred here as a SWM. The SWM that functions as a three-DOF stepper is capable of open-loop orientation control while its rotor spins continuously.
- (2) A CAD/CAE based procedure as a cost-effective way to optimize the design parameters that could significantly affect the torque performance of the VRSM is then presented. This procedure uses a conceptual design as an input to create 3D solid models, upon which FE analyses can be performed to analyze the effects of the key parameters.
- (3) The SWM has been experimentally demonstrated. Preliminary results show that accurate performance can be obtained with open-loop control.

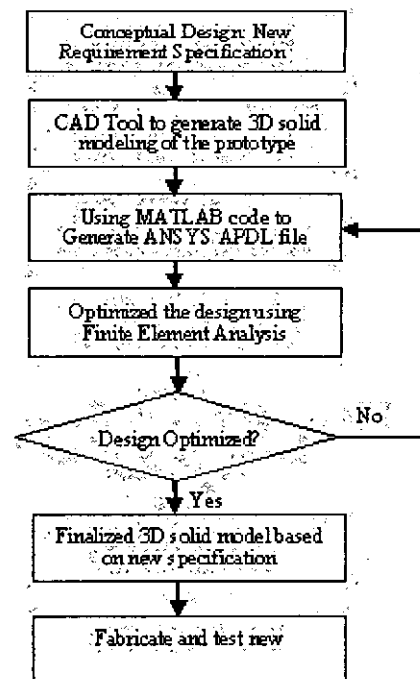


Figure 1: Design approach flowchart for new VRSM prototype

## II CONCEPTUAL DESIGN

The VRSM operates on the principle of variable-reluctance. As illustrated in Fig. 2, a magnetic field is generated when an electrical current flows through the stator EM. A magnetic attraction or repulsion is generated between the stator EM and the rotor (iron or a magnet) pole as the electromagnetic system tries to reduce the reluctance along the magnetic path. The tangential component of the magnetic attraction or repulsion caused the rotor to move.

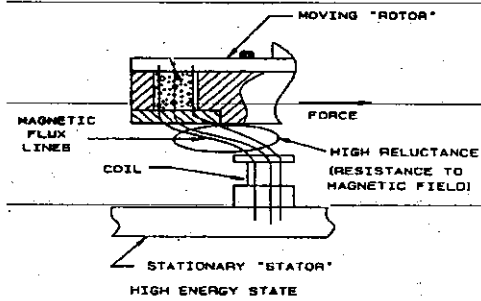


Figure 2: Principle of variable reluctance

In [11], we derived the torque model of a VRSM in the following form:

$$T_k = \frac{1}{2} \mathbf{u}_s^T \frac{\partial [L_{ss}]}{\partial \theta_k} \mathbf{u}_s + \frac{1}{2} \mathbf{u}_r^T \frac{\partial [L_{rs}]}{\partial \theta_k} \mathbf{u}_s + \mathbf{u}_r^T \frac{\partial [L_{rr}]}{\partial \theta_k} \mathbf{u}_r \quad (1)$$

where  $\mathbf{u}$  is the current vector; the subscripts  $r$  and  $s$  denote the rotor and stator respectively;  $k = 1, 2,$  and  $3$  correspond to the  $x, y,$  and  $z$  rotor axes;  $[L_{ss}]$  and  $[L_{rr}]$  are the self inductance sub-matrices of the stator and rotor respectively; and  $[L_{sr}] = [L_{rs}]^T$  is the mutual inductance sub-matrix.

In order to generate no torque corresponding to zero current, the third term on the right side of Eq. (1) must be zero. Thus, we propose to wind the stator electromagnets EM's on non-ferromagnetic cores for the system where permanent magnets (PM) are used as rotor poles. With ferromagnetic cores removed, the self-inductance  $[L_{ss}]$  of the electromagnets is greatly reduced and consequently, the first term of Eq. (1) is small as compared to the second term. The resultant torque, therefore, can be approximated by a linear combination of stator input current, and defined as

$$T_k \approx \mathbf{u}_r^T \frac{\partial [L_{rs}]}{\partial \theta_k} \mathbf{u}_s = [K(\mathbf{q})] \mathbf{u}_s \quad (2)$$

where  $\mathbf{q} = [\alpha \beta \phi]^T$  is a vector of orientation angles defined in the stator reference frame XYZ as shown in Fig. 3.

A particular form of VRSM, referred here as a spherical wheel motor (SWM), offers the ability to spin continuously while the shaft can be tilted arbitrarily from the Z-axis as shown in Fig. 3. The motor is designed to follow the linear relationship suggested by Eq. (2) and can be expressed as a linear combination of three terms:

$$\mathbf{u} = u_\phi (\mathbf{I} + \mathbf{u}_\alpha + \mathbf{u}_\beta) \quad (3)$$

where  $u_\phi$  is a scalar function for the current components responsible for the spin motion about the rotational axis of the shaft;  $\mathbf{I}$  is an identity matrix;  $\mathbf{u}_\alpha$  is a portion of the currents added to  $\mathbf{u}$  for the  $\alpha$  rotation; and similarly  $\mathbf{u}_\beta$  is a portion of the currents for the  $\beta$  rotation.

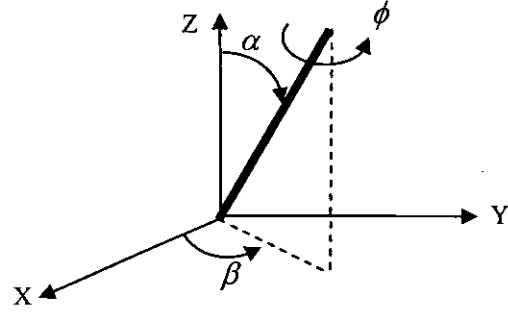


Figure 3: Orientation angles defined in stator frame XYZ

Fig. 4 shows the CAD model of a conceptual SWM. In generating the CAD model, a top-down approach is used. The structure consists of four components; namely, a stator with embedded coils, a rotor with PM's, sensors, and a base containing bearing and cooling units. As shown in Figs. 4(a) and 4(b), the rotor assembly is made of a center block, a rotor shell, and PM's. The lower part of the center block serves as a counter-weight while the top section is a shaft holder where the shaft can be held. On the center block, one or more layers of magnets are placed as shown in Fig. 4(b).

The stator assembly as shown in Figs. (4c), (4d) and (4f) is made of a stator shell and two or more rows of stator EM's. It is desired to fabricate the stator as a complete unit for rigidity, and yet to leave a large opening on the top of the stator shell for ease of assembly – this requirement determines the height of the stator shell. The base provides a support of the rotor assembly, the heat sink for cooling, and the rotor-position/orientation sensors, and together with a cover protects the cabling for the coils and the sensor electronics. The stator is mounted on the base (that supports the rotor by means of a bearing) such that both the stator and the rotor are concentric.

The arrangement of rotor PM's is designed such that adjacent magnets have opposite polarities. The FE analysis is performed for two opposite interacting pairs of the rotor PM's and stator EM's

## III DESIGN ALGORITHM USING ANSYS

To provide an effective means to analyze the effects of the design parameters on the torque performance, a MATLAB code was written to generate the ANSYS command files or APDL (ANSYS Parametric Design Language). These MATLAB codes allow parametric changes in the model directly translate into an APDL file instead of changing the geometric model in Graphic User Interface (GUI). This is

particularly useful for a quasi-static analysis over a range of rotor orientation, where the torque component corresponding to a pole-pair depends on the separation angle and it is necessary to create an APDL file for each of the separation angles over the range of interests. Instead of copying and pasting each section of the APDL file and then modifies the changes the separation angle, the range of separation angles are used as an input to MATLAB code which would compute and generate each quasi-static case in the APDL file for the analysis. It would also prevent modeling errors in CAD when a geometric parameter is changed.

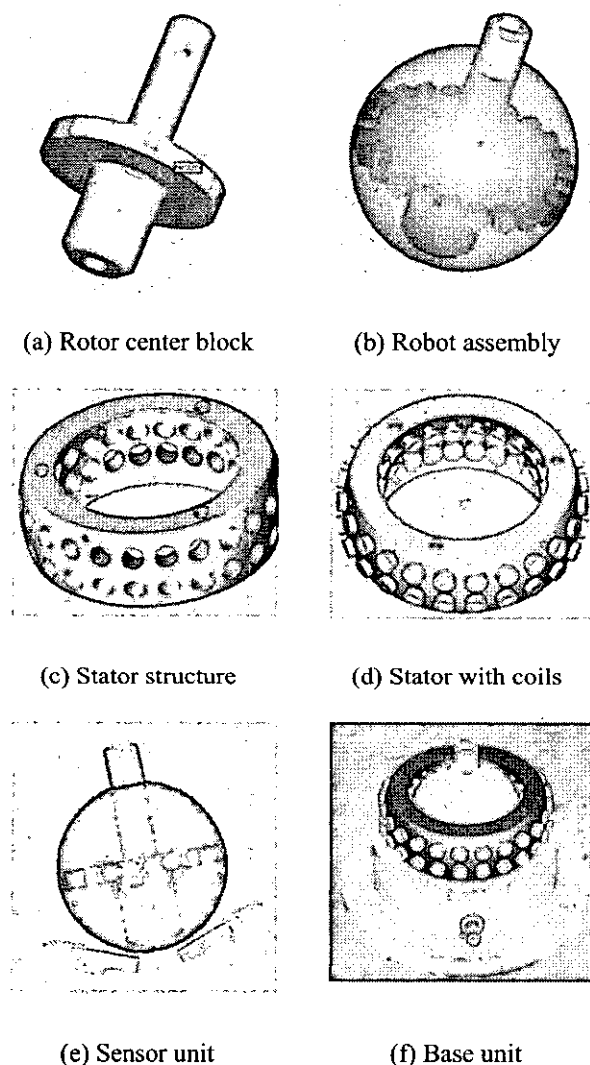


Figure 4: CAD Model of the SWM

#### A. GEOMETRIC MODEL (FIG. 5)

The geometric model begins with modeling of several nodes translated at certain dimensions from the stator reference frame (Fig. 5a). These nodes are used as based position points for modeling of cylindrical shaped rotor poles magnet (Fig. 5b). Then, a larger diameter cylinder is created to model the air gap interaction volume (AGIV) between the rotor PM and stator EM (Fig. 5c), which is created as an

extension of the boundary condition since there is a need for fine meshes in the AGIV. However, the creation of this air-gap volume overlaps the rotor PM. To eliminate the overlapping between these two volumes, Boolean operation was performed to subtract air gap interaction with the rotor PM. The result of the operation created a hole in the air gap interaction as shown in Fig. 5d.

At this point, the rotor PM and AGIV have been modeled (Fig. 5e). The next step involves creating a new coordinate axes that rotated by  $-90^\circ$  degree about z-axis w.r.t. to the world reference frame (WRF) followed by a rotation at  $90^\circ$  about the new x-axis and finally rotation at  $0^\circ$  about the new y-axis. This new coordinate system would be the reference frame for the translated copy of rotor PM and air gap interaction. Another new coordinate axes is created to position the rotor PM and AGIV at the desired Euler angle of rotation. The translation of the rotor and air gap to this new coordinate axes positions the models in the desired position (Fig. 5f).

To model the opposite interaction pair, the same concept used in creating the first rotor PM and air gap interaction is used. In this case, the creation of new coordinate axes would rotate at  $90^\circ$  about z-axis with respect to WRF followed by  $90^\circ$  about new x-axis and  $0^\circ$  about new y-axis. The same translation to the desired correct position is also performed, and the newly created geometric model is shown in Fig. 5g. Since the analysis would be performed on a pair of opposite interaction stator rotor poles pairs, the original rotor PM and AGIV are not longer needed and thus deleted from the model (Fig. 5h).

With the pair of opposite interaction poles pairs modeled, the next step models the polygon of rotor center block. In the conceptual design, the center block is modeled with a shaft support and counter-balance sections. However, those two sections are not modeled in FE analysis since they do not play a role in the FE analysis. In Fig. 5i, the rotor center block is modeled in the WRF. To orient the rotor center block to the end desired position, the similar copy-orient-delete steps as described in creating the two opposite pairs of rotor PM's and AGIV is applied. The resulting model is shown in Fig. 5j.

In the CAD design, the stator is modeled as a hollow sphere but with the top and bottom quarters cut off. In this open hollow sphere are holes where all stator EM's are mounted (Fig. 5k). Holes are modeled as two flat blocks as shown in Fig. 5l. The flat part of block is used as mounting surface or surface for attaching the stator EM. Fig. 5m shows the complete geometric model of the assembly in ANSYS.

The two stator EM's are not modeled because they are elements instead of 3D volumes. A detailed explanation on the stator EM will be described later.

The final step is to define a free space of air as infinite boundary conditions that surround the electromagnetic structure, which is as a rectangular box (Fig. 5n). However, the strongest magnetic scalar potential field occurred in the AGIV and thus, the AGIV is modeled with fine meshes.

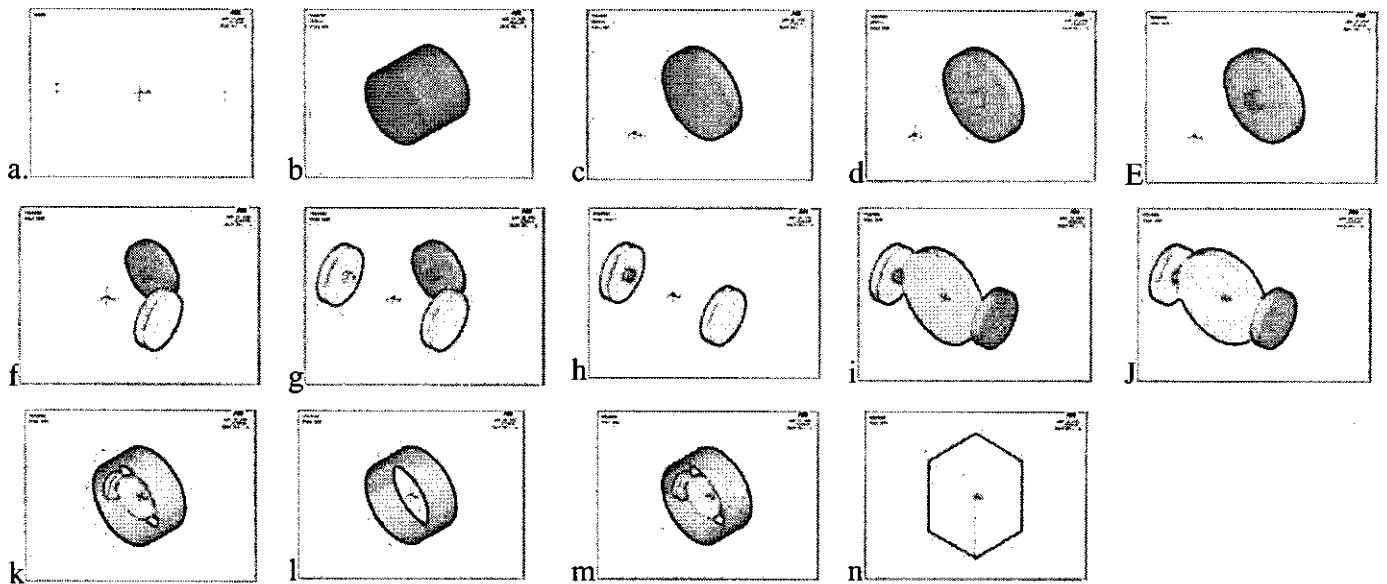


Figure 5 Geometric Modeling Procedure

## B. FINITE ELEMENT ANALYSIS (FIG. 5)

To perform FE Analysis in ANSYS, each part is assigned appropriate element type along with the material property before being meshed. These are often the first several lines of an APDL files or the header.

**Element Type** For the rotor assembly and the stator shell, SOLID 96 element was used, which is an 8-node brick element with 6-DOF including displacement, electric potential, magnetic scalar potential, and temperature. The infinite boundary condition of the free space air volume is modeled using INFIN47 element. This element is a 4-node boundary element that models the far field decay in the magnetic field. The stator EM is modeled as SOURCE36 elements. The attributes of this element would allow model of current source represented as bar, cylindrical or racetrack type. In ANSYS, we model the stator EM as a cylindrical air-cored electromagnet of  $N$  turns.

**Material Properties** The assignment of material properties is specified in term of either relative permeability of BH curves. For free space air region, the relative permeability of  $\mu_r = 1$  is assigned. For the rotor center block made out of iron, we use a relative permeability of  $\mu_r = 1000$ . The relative permeability of rotor PM is obtained from its BH curve, which is the function of the residual magnetization  $B_r$  and the magnitude of coercive force vector  $H_c$ , or in short,  $\mu_r = B_r / \mu_0 H_c$ .

With the assignment of element type and material properties to each part, the model was meshed to finer elements. Fig. 6a shows the meshed elements of the rotor's assembly, which includes the center block and the two magnets. Fig. 6b is the meshed elements of stator assembly, which includes the stator shell and coils. Fig. 6c shows the top view of meshed elements for the whole assembly and Fig. 6d is the corresponding isometric view.

The quality of mesh significantly affects the accuracy of FE solution. The magnetic scalar potential interaction occurred in the volumetric air region between the pairs of rotor and stator poles. Therefore, the air gap interaction volume must be modeled with a fine quality of mesh (Fig. 6e). Finally, the mesh is applied on the infinite free air space boundary conditions (Fig. 6f). Figs. 6g and 6h show the isometric and plane view of the assembly position with respect to the free air space boundary condition in the meshing. Fig. 6i illustrates one quasi-static case. In this case, the rotor assembly is rotated along the Y-axis to define the separation angle. Fig. 6j is an angled view of Fig. 6i to provide a better view of separation angle between the interaction poles.

## IV FABRICATION AND TESTING

To test the concept of a SWM, we modified an existing VRSM [8]. The setup consists of 20 stator EM's (or two layers of 10 coils) and 16 permanent magnets as rotor poles (or two layers of 8 poles) as shown in Fig. 7 and Table 1. The coils are wired in pairs so that two diametrically opposite interaction pair of the rotor poles and stator EMs would yield a common torque as shown in Fig. 6j. In addition, we replaced the three single-axis encoders by four Hall-effect sensors. This eliminates the mechanical guides and thus the associated inertias and friction. Two different magnets were used in this preliminary experiment so that changes can be tested on the existing structure; one measures the spin and the other measures the shaft inclination. We expect that once the open-loop control of the 3-DOF stepper is well understand, there will no need to measure the spin angle of a SWM, which functions essentially as a stepper.

The resolution of a stepping motor are dependent on the number of rotor pole pairs, the number of motor phases (stator EMs) and the drive mode (full or fractional step). An open-

loop switching controller has been developed for a full-step stepping control. Since the rotor poles are evenly spaced at  $45^\circ$  apart, the full-step switching control follows Eq. (4):

$$u_n = f_0 \operatorname{sgn}(\sin \omega_s t) |i_n| \{1 + f_1(\alpha) \cos[(n\pi/5) + f_2(\beta)]\} \quad (4)$$

$$\text{where } n = 1, 2, \dots, 10; f_0 = \begin{cases} (-1)^n & n = 1, \dots, 5 \\ (-1)^{n+1} & n = 6, \dots, 10 \end{cases}$$

$$\text{and } \operatorname{sgn}(x) = \begin{cases} 1 & \text{if } x > 0 \\ 0 & \text{if } x = 0 \\ -1 & \text{if } x < 0 \end{cases}$$

Equation (4) shows that the spin-rate is directly proportional to the frequency of pulses,  $\omega_s$  and the functions  $f_1(\alpha)$  and  $f_2(\beta)$  govern the shaft orientation (or  $\alpha$  and  $\beta$  respectively).

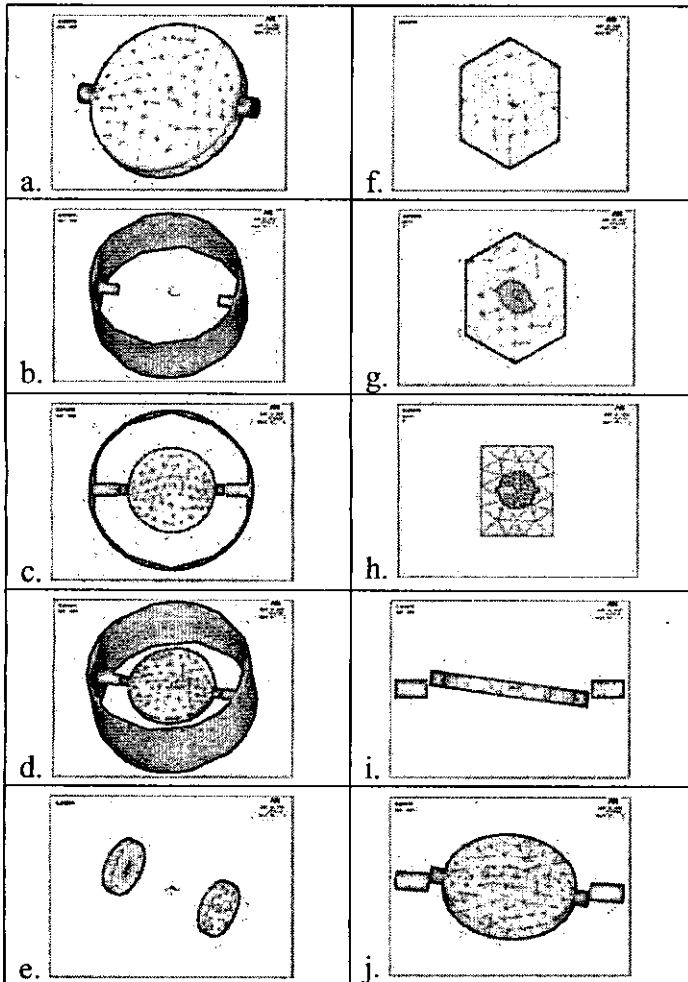
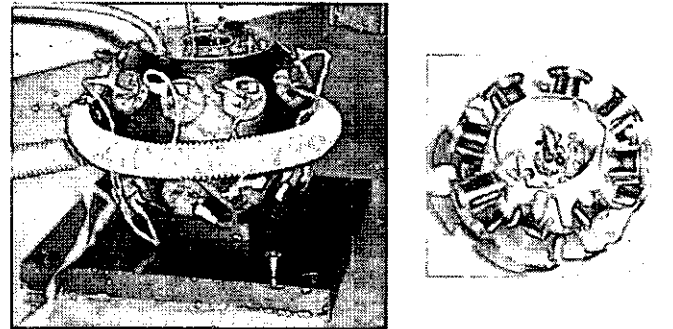


Figure 6: Meshing Procedure

Fig. 8 shows the sensor output (in volts) when the rotor reaches a steady-state spin rate of 340rpm. During initialization, two specified pairs of coils are given a fixed

amount of currents to attract the nearest pairs of rotor PM's such that the shaft aligns with the Z-axis of the stator frame. Fig. 9 shows that the process starts from an initially random inclination, moves to the pre-determined upright position ( $\alpha = \beta = 0, \phi = 90^\circ$ ), and spins to a constant rate of 340rpm. Fig. 10 shows the sensor responses to step change in  $\alpha = 6^\circ$  and  $\beta = 90^\circ$  while the rotor spin at 340rpm about its z-axis.



(a) Stator

(b) Rotor

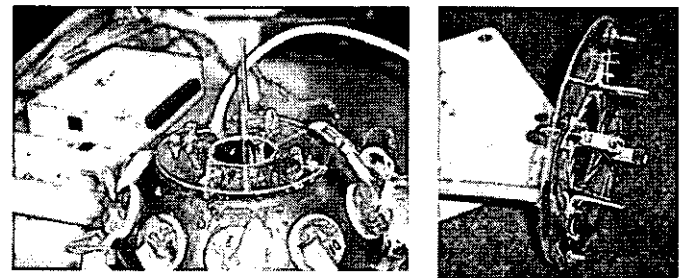


Figure 7: VRSM Prototype

Table 1 SWM test configuration

Stator EMs	20 (2 layers of 10), OD = 0.75 in, 1050 turns
Coil wire	29 AWG
Coil resistance	6.46 Ohms
Rotor PM poles	16 (2 layers of 8), OD=0.5 in
Magnetization axes:	
Stator EMs	$\pm 26^\circ$
Rotor poles	$\pm 20^\circ$

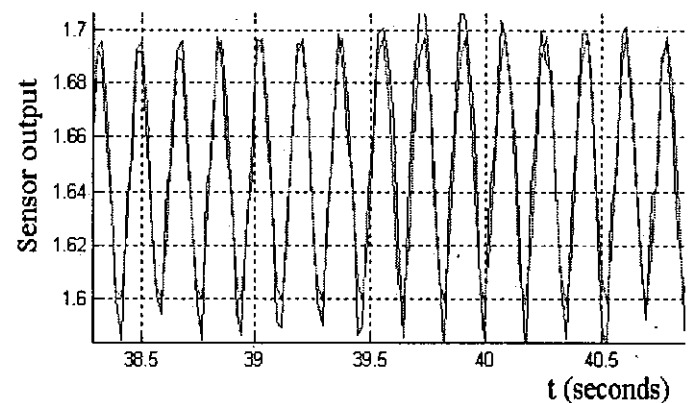


Fig. 8 Steady-state spinning about the Z-axis ( $\alpha = \beta = 0$ ) 340rpm,  $\omega_s = 35.6 \text{ rad/s}$ ,  $i_n = 0.3 \text{ A}$ ,  $f_1(\alpha) = f_2(\beta) = 0$ .  
Solid green line: desired: Dashed blue line: measurement

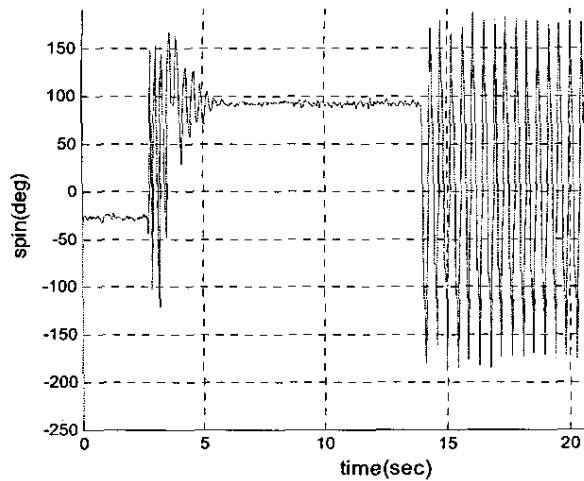


Figure 9 Results illustrating the transient response

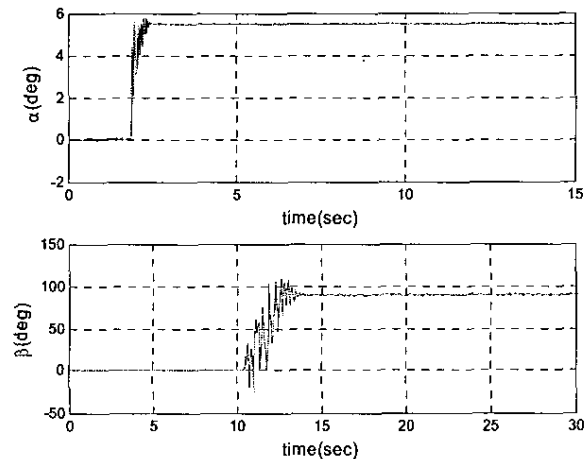


Figure 10 Step change in  $\alpha$  and  $\beta$  while spin at 340rpm

As shown in Figs. 8 and 10, the output of the SWM well matches the measurements in open loop control. The results demonstrate that the SWM functions as a very accurate 3-DOF stepper. The open-loop control shown above, however, does not take into account the dynamics of the motor, which result in a significant lag during the transient. This phase lag is a major factor that could cause the system to become unstable. The dynamic effects, however, can be compensated using feedback control.

## V CONCLUSIONS

We have presented a particular design of VRSM; a SWM that functions as a three-DOF stepper. The SWM is capable of open-loop orientation control while its rotor spins continuously. To offer a cost-effective way to optimize the parameters, we have presented a CAD/CAE based procedure to facilitate the design. Current work uses a conceptual design as an input to create 3D solid models, upon which FE analyses can be performed to optimize key parameters that could significantly affect the torque performance of the VRSM. The SWM has been experimentally demonstrated. Preliminary

results show that accurate performance can be obtained with open-loop control. The design method presented here focuses on predicting the torque generated quasi-statically for motors that have a linear torque-current relationship. The design method, however, does not analyze the motor dynamics, which could result in significant phase lag during transient. This phase lag could significantly affect the motor stability that however can be compensated using feedback control.

## ACKNOWLEDGEMENT

The universe bearing used in the spherical motor prototype was provided by Dr. I-Ming Chen of Nanyang Technological University (Singapore). The authors would like to thank Dr. Wei Lin and Guilin Yang for their technical inputs.

## REFERENCES

- [1] Vachtsevanos, G.J., Davey, K., and Lee, K.M., 1987, "Development of a Novel Intelligent Robotic Manipulator," *IEEE Control Systems Magazine*, June.
- [2] Foggia, A., E. Oliver, F. Chappuis, 1988, "New Three Degrees of Freedom Electromagnetic Actuator," *Conference Record - IAS Annual Meeting*, Vol. 35, New York.
- [3] Hollis, R.L., A.P. Allan, and S. Salcudean, 1987, "A Six Degree-of-freedom Magnetically Levitated Variable Compliance Fine Motion Wrist," Fourth Int'l Symp. on Robotics Research, Santa Cruz.
- [4] Kaneko, K., I. Yamada, and K. Itao, 1988, "A Spherical DC Servo Motor with Three Degrees of Freedom," *ASM Dyn. Sys. & Con. Div.*, Vol. 11, p. 433.
- [5] Neto, L., R. Mendes, and D. A. Andrade, 1995, "Spherical Motor- a 3D Position Servo," *Proc. IEEE Conf. on Electrical Machines and Drives*, 11-13 Sept., pp. 227-231.
- [6] Lee, K.-M. and C.-K. Kwan, 1991, "Design Concept Development of a Spherical Stepper for Robotic Applications," *IEEE Trans. on Robotics and Automation*, Vol. 7, no.1, pp. 175-180, February 1.
- [7] Chirikjian, G. S., & D.Stein, (1999). *Kinematic Design and Commutation of a Spherical Stepper Motor*. IEEE/ASME *Trans. on Mechatronics*, vol. 4, n 4, Piscataway, New Jersey, pp. 342-353.
- [8] Lee, K.-M., R. Roth, and Z. Zhou, 1996, "Dynamic Modeling and Control of a Ball-joint-like VR Spherical Motor," *ASME J. of Dyn. Sys. Measurement and Control*, vol. 118, no. 1, pp. 29-40, March.
- [9] [12] Wang, J., G. Jewel, D Howe, 1998 "Analysis, Design and Control of a Novel Spherical Permanent Magnet Actuator," *IEE Proceedings on Electrical Power Applications*. Vol. 154, no. 1.
- [10] Shigeki, T., Osamu, M., and Guoqiang, Z., 1996 "Development of New Generation Spherical Ultrasonic Motor," *ICRA96*, pp. 2871-2876.
- [11] Lee, K.-M. R. A. Sosseh and Z. Wei, 2004, "Effects of the Torque Model on the Control of a VR Spherical Motor," *IFAC Journal of Control Engineering Practice*, Vol 12/11 pp 1437-1449.
- [12] Sylvester, P. and R. L. Ferrari, 1986, "Finite Elements for Electrical Engineers," Cambridge Univ. Press, New York.
- [13] Seminar notes, 1987, "ANSYS: Magnetic Seminar," Swanson Analysis Systems, Inc., Houston, PA.